A01-30931

AIAA 2001-2205

Coaxial-jet-noise predictions from statistical and stochastic source models

N. Heron, S. Lemaire
Dassault-Aviation
78, quai Marcel Dassault
92214 Saint-Cloud, France

S. Candel
Ecole Centrale Paris
92295 Châtenay-Malabry, France

C. Bailly
Ecole Centrale de Lyon
69131 Ecully, France

7th AIAA/CEAS
Aeroacoustics Conference
28-30 May 2001 / Maastricht, The Netherlands

AIAA 2001-2205

Coaxial-jet-noise predictions from statistical and stochastic source models

Stéphane Lemaire*, Nicolas Héron†
Dassault Aviation, Saint-Cloud 92214 cedex, France

Sébastien Candel‡
École Centrale Paris, Châtenay-Malabry cedex 92295, France

and Christophe Bailly§
École Centrale de Lyon, Ecully cedex 69131, France

Abstract

Two approaches are investigated to predict jet noise and are assessed by comparison of their predictions with experimental data. First, one examines the noise reduction of a jet by the addition of a secondary coaxial jet. A CFD Reynolds Average Navier Stokes-$k-\varepsilon$ computation gives the characteristics of the mean and turbulent flowfields, which are used in two semi-analytical models for noise prediction. One set of calculations extends those developed previously for perfectly expanded free subsonic and supersonic jets. Second, radiation from subsonic and supersonic jets is studied using a stochastic method based on linearized Euler's equations. This method is being developed to simulate the coaxial flows of the first part.

Nomenclature

- a speed of sound,
- D exit nozzle diameter,
- k turbulent kinetic energy,
- M_c convection Mach number,
- S_t Strouhal number $S_t = fD/U$,
- U_c local convection velocity,
- x observer position,
- y local source point,
- ε dissipation rate,
- ρ density,
- ω angular frequency,
- ϕ' local fluctuation of ϕ.

subscripts
- o freestream,
- p primary jet,
- s secondary jet,
- 1 axial direction,
- 2 radial direction.

*Research Scientist, DTA/IAP, 78, Quai Marcel Dassault, Member AIAA
†PhD Student, DPR/ESA, 78, Quai Marcel Dassault
‡Professor of Fluid Mechanics, Laboratoire EM2C, CNRS, Ecole Centrale Paris, Member AIAA
§Assistant Professor, Laboratoire de Mécanique des Fluides et d'Acoustique, CNRS, Ecole Centrale de Lyon, Member AIAA

Introduction

Many coaxial jets aeroacoustic experiments carried out in the past two decades were aimed at finding the best flow configuration for a maximum noise reduction. For subsonic jets,[10] the addition of a coaxial stream reduces the shear with the external flow and results in a direct noise reduction .

For supersonic jets,[13,16] special conditions of temperature and velocity of the secondary jet can eliminate Mach waves generated by the supersonic convection of the turbulent eddies. Because these waves contribute significantly to noise radiation, their suppression could be quite useful.

The aim of this study is to reproduce by two different numerical approaches the results obtained in the experiments of Juvé *et al.*[10] and of Papamoschou.[13,16] The first uses a statistical expression[5,9,17] for noise sources which requires the knowledge of local characteristics of the jet flow, obtained from a Navier Stokes-$k-\varepsilon$ computation. The calculation of noise radiation requires a limited amount of computer ressources. The second method is based on a stochastic description of noise sources and uses the linearized Euler's equations[4] to calculate wave propagation. All the mean flow effects are included in the computation of the acoustic radiation.

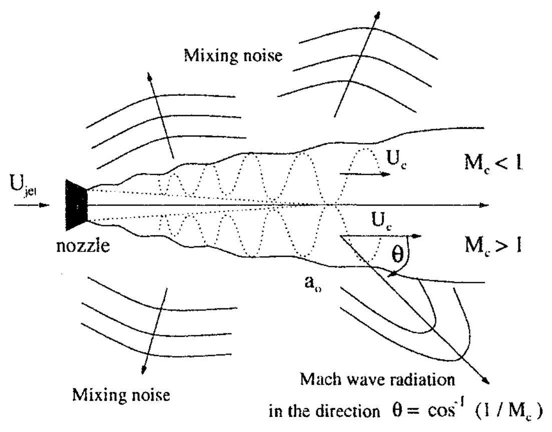

Figure 1: *Acoustic sources in a subsonic jet (top) and in a perfectly expanded supersonic jet (bottom).*

Statistical-source model

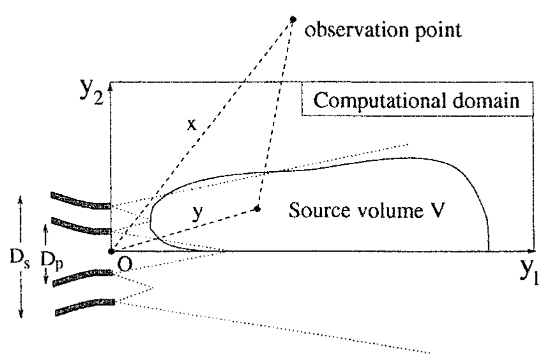

Figure 2: *Acoustic farfield is obtained by a post-processing of an axisymmetrical CFD computation.*

The statistical-source model is derived from Lighthill's analogy. In this framework, the density fluctuations originating from a source volume and detected at a point $\boldsymbol{x}$ in the far field, are given[11] by :

$$\rho'(\boldsymbol{x},t) = \frac{x_i x_j}{4\pi {a_o}^4 x^3} \int_V \frac{\partial^2}{\partial t^2} T_{ij}\left(\boldsymbol{y}, t - \frac{r}{a_o}\right) d\boldsymbol{y} \quad (1)$$

where $r = |\boldsymbol{x} - \boldsymbol{y}|$ and the Lighthill tensor reads $T_{ij} \simeq \rho_o u_i u_j$, if one assumes a high Reynolds number and acoustic generation and propagation without entropy fluctuations.

Defining the density auto-correlation function:

$$C_{pp}(\boldsymbol{x},\tau) = \frac{\overline{(\rho(\boldsymbol{x},t+\tau)-\rho_o)(\rho(\boldsymbol{x},t)-\rho_o))}}{\rho_o {a_o}^{-3}}$$

it is possible to derive expressions for the acoustic intensity:

$$I(\boldsymbol{x}) = C_{pp}(\boldsymbol{x}, \tau = 0)$$

and for the power spectral density:

$$S_{pp}(\boldsymbol{x},\omega) = \frac{1}{2\pi}\int_{-\infty}^{\infty} C_{pp}(\boldsymbol{x},\tau) e^{i\omega\tau} d\tau$$

in terms of the mean flow and turbulent fluctuation correlations.

Using various modeling assumptions one finds that for subsonic jets,[5,6] the sound radiated corresponds to the well-known self- and shear-noise components of the turbulent mixing noise. For supersonic jets,[2,5] one finds in addition a Mach wave noise contribution. The statistical approach requires local values of the mean flow, the velocity fluctuations ($u_t \sim \sqrt{2k/3}$), the characteristic turbulent length ($L_t \sim k^{3/2}/\varepsilon$) and time scale ($\tau_t \sim k/\varepsilon$), the position of the observer (x, θ), the ambient conditions (ρ_o, a_o) and the convection velocity U_c. The determination of this last quantity is a key point in extending the modeling to coaxial configurations. In this geometry there are two shear layers. In each of these regions, the convective Mach number must be evaluated to switch from one acoustic model to the other (mixing noise or Mach wave noise). This choice is made locally. In summary, the model reads in the CFD solution, calculates the axial velocities (for both the primary and the secondary jets), locates shear zones and the potential core of the coflow and determines if the local velocity distribution is that of two jets or that of a single jet, formed by merged primary and coaxial flows. CFD results[7] are presented in figures 6 and 7 in which the turbulent kinetic energy fields used as a marker allow to distinguish the zone with low turbulence level (ambient medium and potential cores) and therefore indicates the presence of one (single flow) or two shear layers (coflow).

Let U_p and U_s be the velocities given by the CFD results along the axes of the jets(centered on the middle of the potential cores), the convection effect is calculated for the internal shear layer with the following expression:[14]

$$M_{cp} = \overline{M_c} + d_{M_c}/\sqrt{1+(a_s/a_p)^2} \quad (2)$$

$$\text{with} \quad \overline{M_c} = \frac{U_p - U_s}{a_p + a_s} \quad \text{and}$$

$$d_{M_c} = \begin{cases} 1.5\overline{M_c} - 0.4 & \overline{M_c} > 0.27 \\ 0 & \overline{M_c} \le 0.27 \end{cases}$$

For the convection Mach number between the secondary jet and the freestream, one may use:[8]

$$M_{cs} = 0.67 \times U_s/a_o \tag{3}$$

Finally, the convection effect is represented either by expressions (2) and (3) respectively for the primary and the secondary shear layer, or only by expression (3) with $M_{cp} = 0.67 \times U_p/a_o$ when the jets are mixed.

Subsonic coaxial jets

Using this statistical model one may first try to retrieve experimental results obtained by Juve et al.[10] For a given subsonic cold jet (U_p = 130 m/s, D_p = 30 mm), two secondary nozzles are considered (D_s = 50 mm and D_s = 100 mm), for a range of velocity ratios ($\lambda = U_s/U_p$). Overall sound pressure levels estimated and measured (figures 3 and 4) are in good agreement. This first set of calculations shows that it is possible to find numerically the speed of the secondary jet which minimizes the noise radiated in the farfield.

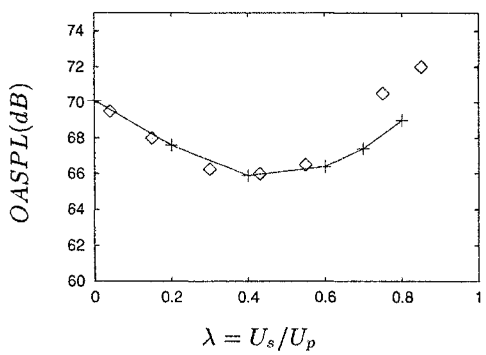

Figure 3: *Overall Sound Pressure Level in dB, θ = 90°, x = 2.5 m, D_p = 30 mm, U_p = 130 m/s and D_s = 50 mm. Experimental data (◇) and numerical predictions(+).*

Supersonic coaxial jets

We now consider supersonic primary jets and attempt to simulate experiments carried out by Papamoschou.[13,16] The goal was to determine which particular secondary coaxial jets could be used to eliminate the Mach waves generated by the primary jet. The principle of this method described in figure 5, consists in setting the secondary jet velocity at a value which brings the convection velocity of the primary jet structures to a subsonic value with respect to the sound speed in the secondary jet.

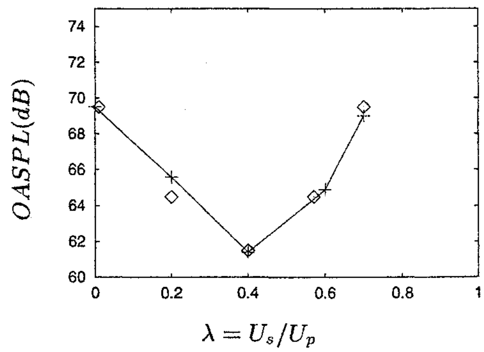

Figure 4: *Overall Sound Pressure Level in dB, θ = 90°, x = 2.5 m, D_p = 30 mm, U_p = 130 m/s and D_s = 100 mm. Experimental data (◇) and numerical predictions(+).*

Case	M_p	$\frac{T_p}{T_o}$	M_s	$\frac{T_s}{T_o}$	$\frac{\dot{m}_s}{\dot{m}_p}$	$\frac{F_{p+s}}{F_p}$
A	1.5	2.8	0.00	1.0	0	1.00
B	1.5	2.8	0.83	1.7	2.1	1.92

The computational results are briefly illustrated in figures 6 and 7. The influence of the secondary jet is clearly visible with the extension of the potential core and the modification of the turbulent kinetic energy field.

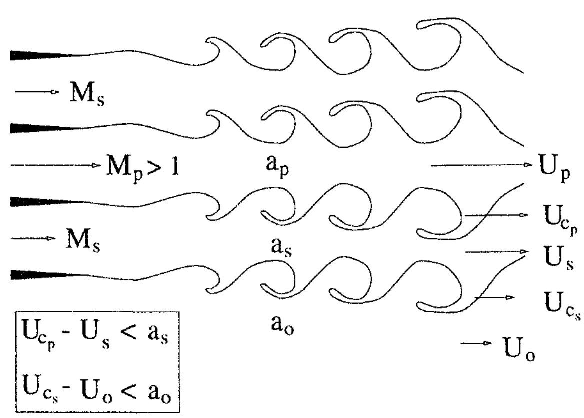

Figure 5: *Principle of the Mach wave noise elimination method by Papamoschou:[13] for a given primary jet, the secondary jet must respect the boxed conditions.*

Results of calculations given in figure 8 are in agreement with the experimental data. The noise reduction is not very important in case B relative to case A. This can be explained by the fact that the eddies near the nozzle are not supersonic relative to the sound speed of the secondary jet, but only relative to the ambient sound speed, once the jets are mixed. Like Papamoschou,[15] we note that the secondary jet has not eliminated, but only shifted the zone of Mach wave generation(figure 9), because of

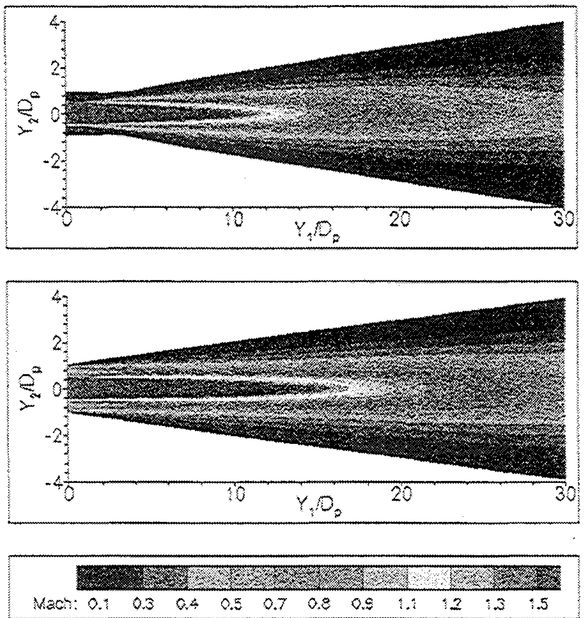

Figure 6: *Mach number fields for cases A and B.*

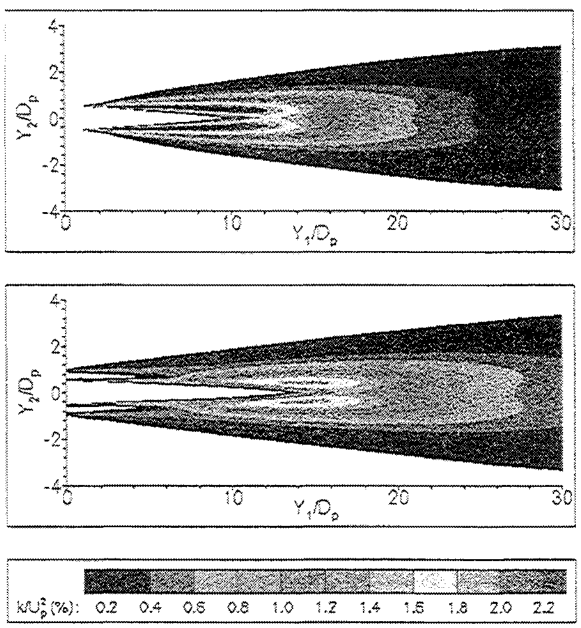

Figure 7: *Turbulent kinetic energy fields for cases A and B.*

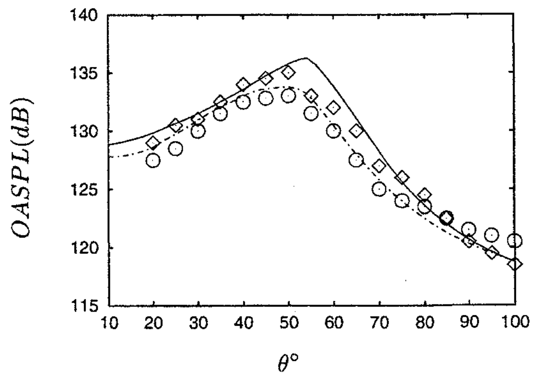

Figure 8: *Acoustic directivity in dB as a function of the outlet angle θ. Experimental data ($\diamond$/$\odot$) and numerical predictions (——/— · —) for case A/B.*

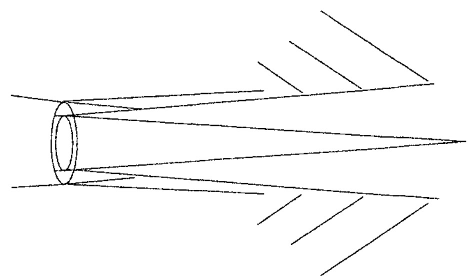

Figure 9: *Papamoschou's experiment:*[15] *In case B, coaxial jet conditions eliminate near field Mach waves, but stretches the potential core, resulting in Mach wave emission from the untreated far field.*

the stretching of the primary potential core. One should note however that the thrust in case B is twice that corresponding to A.

Stochastic-source model

A second approach to the problem relies on the linearized Euler equations (LEE) and uses a stochastic description of the noise sources[4].[3] All terms involved in Navier-Stokes equations are linearized around a mean steady flow and cast in the left hand side while one keeps only quadratic turbulent fluctuations in the Reynolds tensor as source terms on the right hand side. Details about the definition of the source terms can be found in Bailly *et al.*[1] This allows a decoupling between the determination of the acoustic sources and the propagation in the far-field of the disturbances created by these sources. All the interactions between the acoustic field and the mean flow are included in the propagation term. This is contrary to Lighthill's formulation where these effects are included in the source term (Lighthill's tensor) and need to be modeled. To limit the requirements in computer ressources, we use an axisymmetric formulation. The linearized Euler equations with source term read, in cylindrical coordinates :

$$\frac{\partial U}{\partial t} + \frac{\partial E}{\partial z} + \frac{\partial F}{\partial r} + H + J = S$$

where the unknown vector is :

$$U = \begin{pmatrix} \rho' \\ \rho_0 u' \\ \rho_0 v' \\ p' \end{pmatrix}$$

The flux vectors are :

$$E = \begin{pmatrix} \rho' u_0 + \rho_0 u' \\ u_0 \rho_0 u' + p' \\ u_0 \rho_0 v' \\ u_0 p' + \gamma p_0 u' \end{pmatrix}, \; F = \begin{pmatrix} \rho' v_0 + \rho_0 v' \\ v_0 \rho_0 u' \\ v_0 \rho_0 v' + p' \\ v_0 p' + \gamma p_0 v' \end{pmatrix}$$

and

$$H = \begin{pmatrix} 0 \\ (\rho_0 u' + \rho' u_0)\dfrac{\partial u_0}{\partial z} + (\rho_0 v' + \rho' v_0)\dfrac{\partial u_0}{\partial r} \\ (\rho_0 u' + \rho' u_0)\dfrac{\partial v_0}{\partial z} + (\rho_0 v' + \rho' v_0)\dfrac{\partial v_0}{\partial r} \\ (\gamma - 1)\left(p'\dfrac{\partial u_0}{\partial z} + p'\dfrac{\partial v_0}{\partial r} - u'\dfrac{\partial p_0}{\partial z} - v'\dfrac{\partial p_0}{\partial r}\right) \end{pmatrix}$$

The geometrical source term is given by :

$$J = \begin{pmatrix} \dfrac{\rho_0 v'}{r} + \dfrac{\rho' v_0}{r} \\ 0 \\ 0 \\ \dfrac{\gamma p' v_0}{r} + \dfrac{\gamma p_0 v'}{r} \end{pmatrix}$$

S represents the turbulent sources and will be described later in the paper.

Discretization

The finite difference scheme of Tam and Webb[20] is used to discretize the previous equations. This scheme has low dispersive and dissipation characteristics. Accurate non reflecting boundary conditions of Tam and Dong[19] are used to simulate an infinite domain. The jet axis is treated in an appropriate manner which consists in replacing the terms of the form $\frac{\Phi}{r}$ by $\frac{\partial \Phi}{\partial r}$. In case of a supersonic inflow (mean flow), all fluctuations are forced to zero at the inflow boundary.

Source term

The turbulent source terms read :

$$S = \begin{pmatrix} 0 \\ \overline{u_t \dfrac{\partial u_t}{\partial z}} + \overline{v_t \dfrac{\partial u_t}{\partial r}} - u_t \dfrac{\partial u_t}{\partial z} - v_t \dfrac{\partial u_t}{\partial r} \\ \overline{u_t \dfrac{\partial v_t}{\partial z}} + \overline{v_t \dfrac{\partial v_t}{\partial r}} - u_t \dfrac{\partial v_t}{\partial z} - v_t \dfrac{\partial v_t}{\partial r} \\ 0 \end{pmatrix}$$

where $\overline{\Phi}$ stands for the ensemble average of the turbulent quantity Φ, u_t and v_t are turbulent components of the velocity field. The Stochastic Noise Generation and Radiation (SNGR) model is used to obtain a synthetized velocity field. The SNGR model is built up from a finite sum of Fourier modes :

$$\boldsymbol{u}_t(\boldsymbol{x}, t) = 2\sum_{n=1}^{N} \tilde{u}_n \cos[\boldsymbol{k}_n \cdot (\boldsymbol{x} - \boldsymbol{U}_c t) + \psi_n + \omega_n t]\boldsymbol{\sigma}_n$$

where N is the number of Fourier modes, $\tilde{u}_n$ is the amplitude of the n^{th} mode, $\boldsymbol{\sigma}_n$ is a unit vector. $\boldsymbol{U}_c$ is the local convection velocity of the turbulent eddies. ω_n is the random temporal frequency of the n^{th} mode and its probability density is taken as a Gaussian function centered around $\omega_n^0 = 2\pi\varepsilon/k$. All the other quantities are chosen by assuming that the local turbulent fluctuations may be described as an homogeneous and isotropic field of fluctuations.

$$\tilde{u}_n = \sqrt{E(\mathrm{k_n})\Delta \mathrm{k_n}}$$

in order to have $k = \sum_{n=1}^{N} \tilde{u}_n^2$ which approximates $k = \int_0^{+\infty} E(\mathrm{k})d\mathrm{k}$ where $E(\mathrm{k})$ is the kinetic energy spectrum. A Von Karman spectrum is used in this work. The norm of the wave vector $\boldsymbol{k}$ lies within $\mathrm{k_{min}}$ and $\mathrm{k_{max}}$ where $\mathrm{k_{max}}$ is determined by the smallest wavelength that can be resolved by the numerical scheme and $\mathrm{k_{min}}$ is a wave number which is linked to the most energetic eddies. The discretization reads :

$$\mathrm{k_n} = \mathrm{k_{min}}\, e^{(n-1)\Delta \mathrm{k_0}}, \forall n = 1, \cdots, N$$

with :

$$\Delta \mathrm{k_0} = \frac{\ln \mathrm{k_{max}} - \ln \mathrm{k_{min}}}{N - 1}$$

Numerical procedure

The procedure used for the computation of LEE with the SNGR model is as follows :

1. First, a Navier-Stokes $k - \varepsilon$ steady calculation is carried out to get the mean flow for the LEE, k and ε which are needed to calculate the source terms S (amplitudes and spectral characteristics). The Dassault-Aviation Navier-Stokes code AETHER has been used to solve the RANS equations on an unstructured finite element mesh.

2. The previous results are interpolated on an acoustic grid adapted to the solution of the LEE. The cell size is directly linked to the smallest wavelength to be resolved. The domain must also extend far enough to get accurate radiation boundary conditions and an accurate acoustic far field.

3. Finally, the LEE are solved on the acoustic mesh with the explicit time dependent scheme described earlier.

Application to subsonic jet noise

Radiation from a subsonic free jet is calculated using the linearized Euler equations with SNGR model. The jet Mach number M_j is 0.86 with a nozzle diameter D_j equal to 2.5 cm. The temperature ratio T_j/T_o is equal to 1. These values correspond to experimental data[12] with a Reynolds number based on the jet charateristics of 4.9×10^5. The acoustic computational domain comprises 667 and 414 points in the axial and radial directions respectively and is centered at the end of the potential core. The grid spacing is uniform and equal to 1.5 mm ($\simeq D/17$). Frequencies up to 34,7 Hz ($St = 2.9$) may be resolved with these parameters. Pressure time histories are computed along a circle of radius equal to 24 D_j. The total simulated time is equal to 0.02 seconds (10000 time steps). This record length defines the low frequency limit of this calculation which is approximately 500 Hz ($St = 0.05$). One hundred Fourier modes are used for the stochastic source modelling ($N = 100$).

The unsteady pressure field at time t=0.02s is represented in figure 10, the angular distribution of normalized sound pressure is shown in figure 11 and the normalized acoustic spectrum for an observer located at $\theta = 90^o$ is given in figure 12. Computational results are compared to experiments of Lush[12] and Tanna.[21] The level of pressure fluctuations is of the same order as the experimental data, the directivity obtained numerically differs from experimental values of Lush between 70 and 110^o and from experimental values of Tanna at 40^o. It also differs for small angles below 20 degrees. The shape of the acoustic spectrum at 90^o is well retrieved by the computation except in the low frequency range ($St < 0.2$). One should not except a perfect match between the data and the present estimates because the calculations are axisymmetric and the farfield condition is not exactly fulfilled.

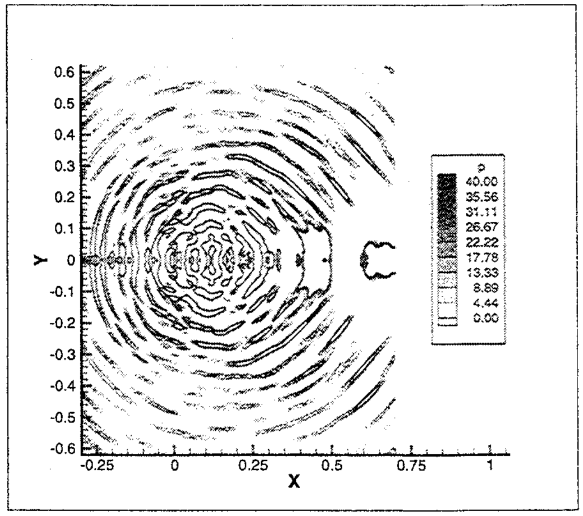

Figure 10: *Snapshot of the pressure field, M_j=0.86, D_j=2.5 cm, T_j/T_o=1, t=0.02 s*

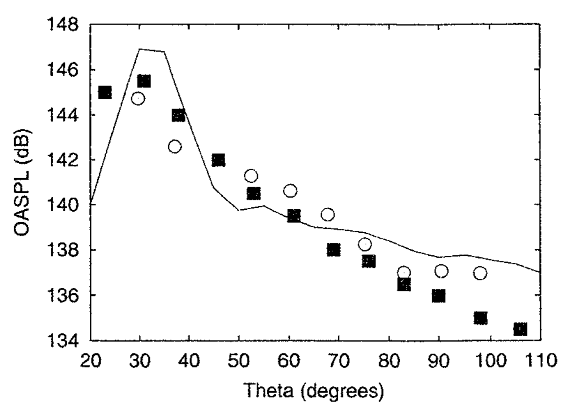

Figure 11: *Angular distribution of normalized sound pressure levels (OASPL), numerical results (——), experimental results of Lush(■) and Tanna(○)*

Application to supersonic jet noise

A supersonic jet case is also investigated with the LEE+SNGR procedure. The jet is again perfectly expanded with a temperature ratio T_j/T_o equal to 1. The Mach number is $M_j = 2$ and the nozzle diameter is equal to 4 cm. The acoustic computational domain comprises 700×550 points with an uniform grid spacing of 2 mm

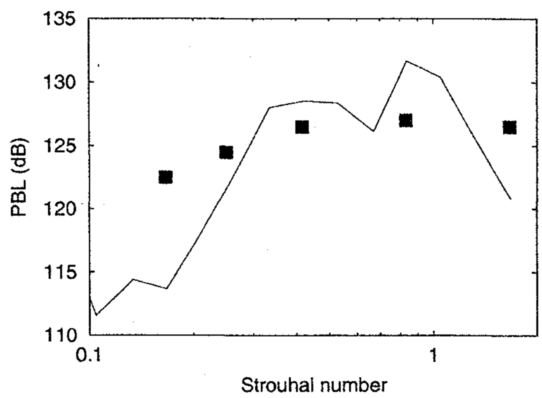

Figure 12: *Spectral content of normalized sound pressure levels for $\theta = 90^o$ as a function of the Strouhal number, numerical results(——) and experimental results of Lush(■)*

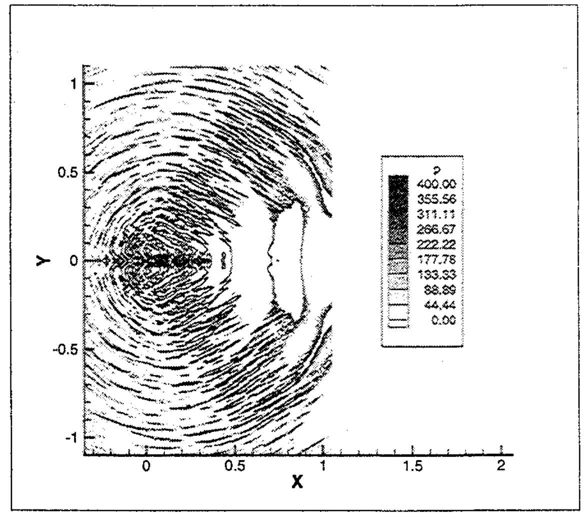

Figure 13: *Snapshot of the pressure field, M_j=2, D_j=4 cm, T_j/T_o=1, t=0.052 s*

($D_j/20$) allowing to resolve frequencies up to 25 kHz ($St = 1.43$). The pressure is observed at a radial distance of 25 D_j. The total record length is equal to 0.052s (40000 time steps) providing information on frequencies exceeding 200 Hz ($St = 0.01$). One hundred Fourier modes are used in the stochastic description of the turbulent source field.

To comply with the fact that Seiner's acoustic measurements are carried out at 30 diameters from the nozzle exit, the numerical estimates are extrapolated to this nozzle distance and to the corresponding angles. Instability waves are clearly identified in figure 13 along with the highly directional Mach waves. The directivity of the angular distribution of the normalized acoustic intensity is represented in figure 14. Computational results are compared to data of Tanna[21] and Seiner.[18] The OASPL distribution is well retrieved except at small angles ($\theta < 30^o$). This is due to the strong instabilities which develop near the jet axis and which are amplified by the linearized Euler formulation.

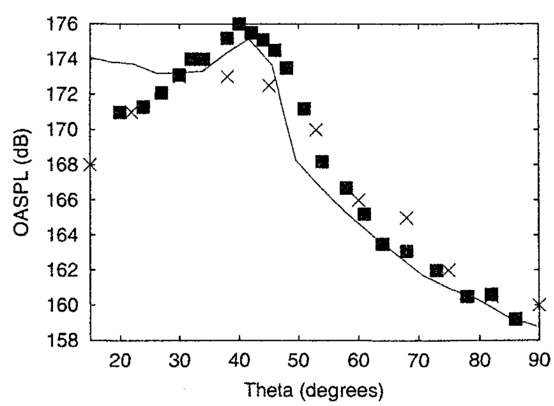

Figure 14: *Angular distribution of normalized sound pressure levels (OASPL), numerical results(——), Tanna(×) and Seiner(■) experimental results*

Conclusion

A statistical model has been used to calculate the acoustic farfield generated by coaxial jets. Based on a numerical estimation of the acoustic sources and of their local convection velocity, this method gives reasonably accurate subsonic and subsonic/supersonic flow noise predictions at a very low computational cost. This method is readily applicable to practical problems but needs some corrections to include refraction effects and is limited to free shear flows.

In a second procedure, acoustic predictions are obtained with the coupled LEE+SNGR method. This has promise for a future application to subsonic and supersonic coaxial jets. Results are at this point preliminary and further refinements are needed. The main issue will be to improve the axisymmetric formulation of the stochastic source terms but one should notice that the axisymmetric framework will still remain approximative and that only a three dimensional formulation should be able to account for an accurate far field.

Acknowledgements

The authors wish to thank Dr. Frederic Chalot and Dr. Michel Ravachol from Dassault-Aviation CFD team for fruitful discussions.

References

[1] C. Bailly, C. Bogey, and D. Juvé. Computation of flow noise using source terms in linearized euler's equations. *AIAA Paper 2000-2047.*

[2] C. Bailly, S. Candel, and P. Lafon. Prediction of supersonic jet noise from a statistical acoustic model and a compressible turbulence closure. *Journal of Sound and Vibration*, 194(2):219–242, 1996.

[3] C. Bailly and D. Juvé. A stochastic approach to compute subsonic noise using linearized euler's equations. *AIAA Paper 99-1872.*

[4] C. Bailly, P. Lafon, and S. Candel. A stochastic approach to compute noise generation and radiation of free turbulent flows. *16th AIAA Aeroacoustics Conference*, 1995.

[5] C. Bailly, P. Lafon, and S. Candel. Subsonic and supersonic jet noise predictions from statistical source models. *AIAA Journal*, 35(11), 1997.

[6] W. Béchara, P. Lafon, C. Bailly, and S. Candel. Application of a k-ϵ turbulence model to the prediction of noise for simple and coaxial free jets. *J. Acoust. Soc. Am.*, 97(6):3518–3531, 1995.

[7] F. Chalot, M. Mallet, and M. Ravachol. A comprehensive finite element navier-stokes solver for low and high-speed aircraft design. *32nd Aerospace Sciences Meeting and Exhibit*, 1994.

[8] P.O.A.L. Davies, M.J. Fisher, and M.J. Baratt. The characteristics of the turbulence in the mixing region of a round jet. *Journal of Fluid Mechanics*, 15:337–367, 1963.

[9] J.E Ffowcs Williams and G. Maidanik. The mach wave field radiated by supersonic turbulent shear flows. *Journal of Fluid Mechanics*, 21(4):641–657, 1965.

[10] D. Juvé, J. Bataille, and G. Comte-Bellot. Bruit des jets coaxiaux froids subsoniques. *Journal de Mécanique Appliquée*, 2(3):385–398, 1978.

[11] M.J. Lighthill. On sound generated aerodynamically, i. general theory. *Proceedings of the Royal Society of London*, 211:564–587, 1952.

[12] P.A. Lush. Measurements of subsonic jet noise and comparison whith theory. *Journal of Fluid Mechanics*, 46:477–500, 1971.

[13] D. Papamaschou. Mach wave elimination in supersonic jets. *AIAA journal*, 35(10):1604–1611, 1997.

[14] D. Papamoschou and A. Bunyajitradulya. Evolution of large eddies in compressible shear layers. *Physics of Fluids*, 9(3):756–765, 1997.

[15] D. Papamoschou and M. Debiasi. Targeted mach wave elimination. *AIAA Paper 2000-0085.*

[16] D. Papamoschou and M. Debiasi. Noise measurements in supersonic jets treated with the mach wave elimination method. *AIAA Journal*, 37(2):154–160, 1999.

[17] H.S. Ribner. The generation of sound by turbulent jets. *Academic Press*, VIII:103–182, 1964.

[18] J.M. Seiner and M.K. Ponton. The effects of temperature on supersonic jet noise emission. *DGLR-AIAA Paper 92-02-046.*

[19] C.K.W. Tam. Advances in numerical boundary conditions for computational aeroacoustics. *AIAA Paper 97-1774.*

[20] C.K.W. Tam. Computational aeoracoustics: issues and methods. *AIAA 95-0677*, 1995.

[21] H.K. Tanna, P.D. Dean, and M.J. Fisher. The influence of temperature on shock-free supersonic jet noise. *Journal of Sound and Vibration*, 39(4), 1975.